—Brief Paper—

DESIGN OF ANTI-SLIP CONTROLLER FOR AN ELECTRIC VEHICLE WITH AN ADHESION STATUS ANALYZER BASED ON THE EV SIMULATOR

Lianbing Li, Shinya Kodama, and Yoichi Hori

ABSTRACT

The In this paper, a simulator of a one-wheel Electric Vehicle system is designed for testing an anti-slip controller using the Motor-Generator system. The drive motor of the M-G system is used to simulate the drive wheel of the Electric Vehicle, and the load motor is used to simulate the load force of the chassis. In the driving process, the torque of the load motor is changed according to the drive force of the chassis that is calculated by the program. So it can simulate the dynamic process of the tire-road system. Based on this simulator system, an anti-slip controller based on an Adhesion Status Analyzer is proposed. Information about the wheel speed is acquired by using a Back EMF Observer. A load torque disturbance observer is designed to stabilize the acceleration of the wheels. The Adhesion Status Analyzer is used to generate safe acceleration commands for the anti-slip controller. When a slip occurs, the anti-slip controller will decrease the torque quickly, and at the same time, by estimating the dynamic status of adhesion, the Adhesion Status Analyzer will restrain the acceleration command within a safe area. The effectiveness of the proposed approach is verified by using the EV slip simulator.

KeyWords: EV, anti-slip control, adhesion.

I. INTRODUCTION

The adhesion characteristics between a tire and road surface have great effects on the driving and braking control of a vehicle. In order to acquire high-performance motion characteristics, the traction force of the engine or motor should be regulated to maintain a good adhesion status. This means that the vehicle stability and safety can be improved through drive torque control. In order to acquire better adhesion performance under any road conditions, a slip prevention controller is needed. A slip caused by accelerating, decelerating or braking usually leads to unsafe motion of the vehicle. To prevent slips, many technologies have been developed, such as Model Following Control (MFC) [1,2], and optimal slip ratio control [3]. Sliding mode measurement feedback control [4], and slip ratio fuzzy control [5] also have achieved fine results in slip control. Current disturbance observers also can be used to limit the increase in wheel speed [6]. Slip controllers based on disturbance observers [7] or road conditions estimators [3,8] have also been studied recently. In this paper, a novel controller scheme based on an observer of the inertia moment is proposed.

In fact, the testing of skid controllers is difficult and expensive. Commonly, real vehicles, real slippery roads and other expensive equipment are needed to test the valid-

Manuscript received April 20, 2005; revised January 26, 2006, accepted May 15, 2006.

Lianbing Li is with the Department of Electrical Engineering Hebei University of Technology (e-mail: lilianbing@horilab.iis.u-tokyo.ac.jp).

Shinya Kodama is with the Technical Center Toyota Motor Corporation (e-mail: kodama@horilab.iis.u-tokyo.ac.jp).

Yoichi Hori is with the Institute of Industrial Science University of Tokyo (e-mail: hori@iis.u-tokyo.ac.jp).

ity of a slip controller. In this paper, a simulator of a one-wheel Electric Vehicle (EV) system is proposed for testing slip prevention controllers using the M-G set. The drive motor of the M-G setup is used to simulate the drive wheel of the EV, and the load motor is used to simulate the load force of the chassis. In the driving process, the torque of the load motor is changed according to the drive force of the chassis that is calculated by the program. So it can simulate the dynamic process of the tire-road system. Based on this simulator system, a novel slip control method is proposed and has been tested. The simulation results obtained with MATLAB and experiment results have the same features, and the results verify the simulation performance of the M-G system. The experiment results prove the validity of the slip controller.

II. VEHICLE DYNAMIC MODEL

The problem of wheel slip control can be analyzed by using a one-wheel-car model [4] as shown in Fig. 1. There are two inertias in this system, the rotating wheel and the body of the car. The dynamic equation of the system can be expressed as

$$\dot{\omega} = \frac{T - F_d r - F_w(\omega) r}{J_w}, \tag{1}$$

$$\dot{V} = \frac{F_d - F_V(V)}{M}, \tag{2}$$

where T is the sum of the driving and braking torques, *i.e.*, $T = T_d - T_b$; F_d is the drive force of the chassis; F_w is the average friction force of the driving wheels for acceleration and the average friction force of all wheels for deceleration; F_V is the wind force of the vehicle. M is the mass of the chassis and the wheels of the vehicle, *i.e.*, $M = M_v + M_w$.

The slip ratio λ is used to describe the slip status between the road and tire. It is defined as

$$\lambda = \frac{V_W - V}{V_W} \quad \text{(driving)}, \tag{3}$$

$$\lambda = -\frac{V - V_W}{V} \quad \text{(braking)}, \tag{4}$$

where V_W is the wheel speed, and V is the velocity of the chassis.

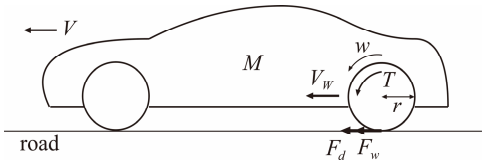

Fig. 1. One-wheel vehicle model.

The friction coefficient μ is a function of slip ratio λ, $\mu = f(\lambda)$, which is dependent on the road conditions. For different conditions of the road, such as dry, wet, snowy, etc., the relationship between λ and μ is different.

The drive force of the vehicle F_d is proportional with the friction coefficient and the pressure on the road.After the friction coefficient μ is found from the slip ratio λ by using the $\mu - \lambda$ curve, the driving force F_d can be calculated by

$$F_d = N\mu(\lambda), \tag{5}$$

where N is the normal component of the reactive effect on the tires. A block diagram of the vehicle is shown in Fig. 2.

III. THE WHEEL DYNAMIC SIMULATOR USING THE M-G SETUP

Based on the block diagram shown in Fig. 2, a vehicle simulator using the M-G set can be designed as shown in the block diagram in Fig. 3. The slip ratio λ of the vehicle system can be calculated based on the speed of the wheel and the chassis. According to the simulated road status, such as dry, wet, or icy road, ramp road, and so on, the friction coefficient and the load torque as well as the load current can be calculated.

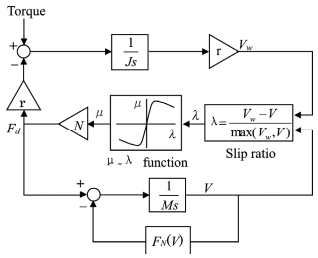

Fig. 2. Block diagram of the vehicle.

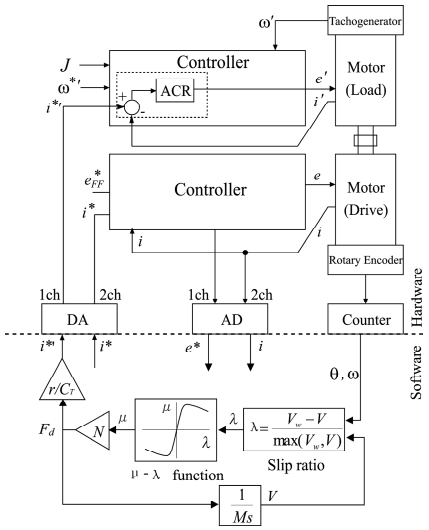

Fig. 3. Block diagram of the vehicle simulator based on the M-G set.

For four kinds of conditions, (A) normal asphalt road, (B) slippery road, (C) ramp up road, and (D) ramp down road, the vehicle simulator was tested, and the experimental results are shown in Fig. 4.

The parameters, such as the inertia moment of the wheel and the chassis, can be adjusted freely to adapt to different vehicle characteristics. At the same time, friction and wind resistance can also be simulated by the system. Here, these disturbances were ignored in the simulation and experiment.

IV. SLIP PREVENTION SCHEME UTILIZING THE CHARACTERISTIC OF BACK-EMF

4.1 Back EMF observer

When there is no speed sensor, the slip prevention controller can also be realized with other signals such as the back EMF (ElectroMotive Force). This kind of slip controller may have greater reliability and more robust performance. But the signal of the back EMF cannot be detected directly, so it is necessary to set up an observer to estimate the value of the back EMF. A current disturbance observer with variable gain and time constant was discussed in [6], where the torque drop characteristic was used to limit the torque when a slip occurred. The current dis turbance observer was used to compensate for the voltage drop caused by the back EMF, so in fact it was also a back EMF observer. In this paper, it is employed to estimate the back EMF, and with the EMF signal, the acceleration also can be acquired as shown in Fig. 5.

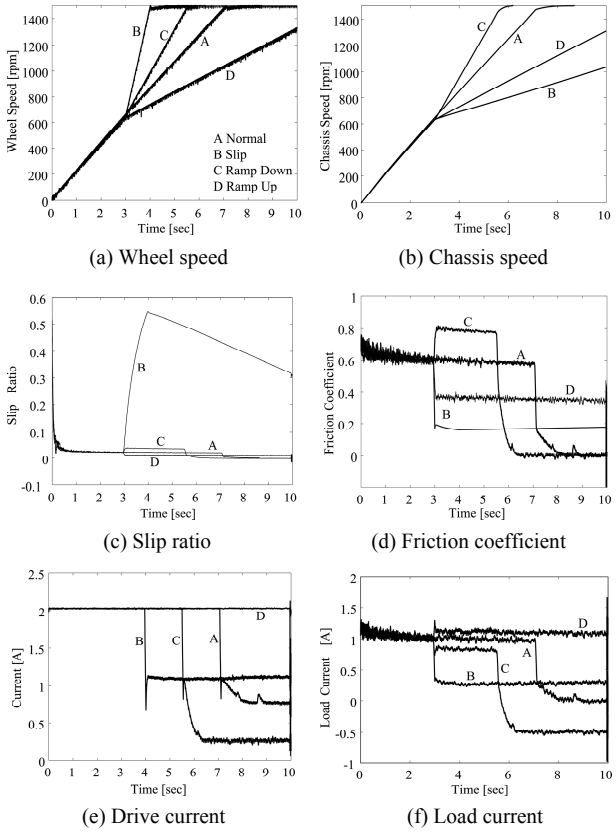

(a) Wheel speed (b) Chassis speed

(c) Slip ratio (d) Friction coefficient

(e) Drive current (f) Load current

Fig. 4. Experiment results obtained with the vehicle simulator under different road conditions.

The estimated back EMF can be expressed as

$$\hat{V}_{emf} = \frac{u^* - (Ls + R)i}{\tau s + 1}. \tag{6}$$

The acceleration can be expressed as

$$\hat{a} = \frac{\hat{V}_{emf}(J_n / C^2)s}{\tau_1 s + 1}, \tag{7}$$

where $1/\tau s + 1$ and $1/\tau_1 s + 1$ represent a low-pass filter for restraining the noise of the estimated value. J_n is the normal value of the equivalent inertia of the vehicle on its wheel.

In the inner loop of the controller, an appropriate current regulator (ACR) is designed to follow the current command quickly.

4.2 Nonlinear noise filter of the observed back EMF

In order to deal with the noise problem in the observed back EMF or other signals, a novel filter is designed as shown in Fig. 6. It is applicable if the original signal without noise is differentiable. If the limit1 is regulated with the true differential value, better performance may be achieced.

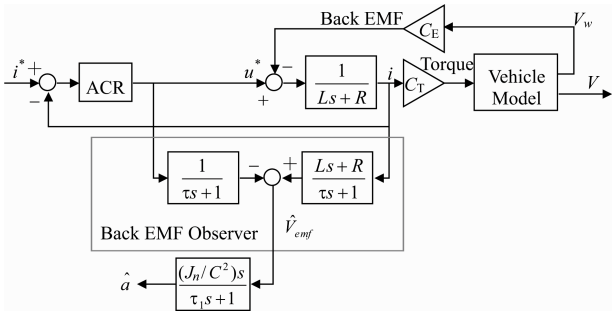

Fig. 5. The acceleration observer.

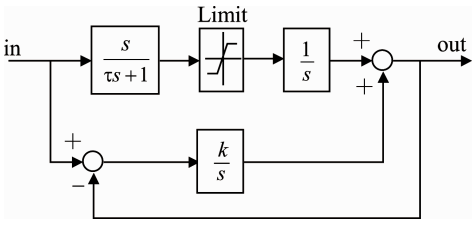

Fig. 6. Block diagram of the nonlinear filter.

The simulation curves obtained using the novel filter are shown in Fig. 7. Compared with the normal low-pass filter, it shows special merits. There is no large time delay, and the curve is smooth when the proposed filter is used. The experimental curves shown in Fig. 8 have the same feature as the simulation curves.

4.3 The slip prevention scheme based on the load torque observer with back EMF

With necessary information about acceleration, it is possible to construct a load torque observer, as shown in Fig. 5. With this approach, the load torque disturbance can be observed without a speed sensor. In Fig. 5, since the current is proportional to the torque, the load torque expressed by its current i_L, and i_d is the induced current of F_d.

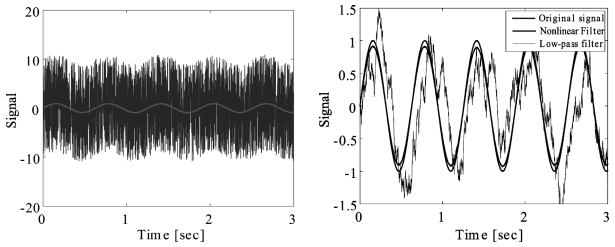

(a) Original and noised signal (b) Comparison of the curves

Fig. 7. Simulation curves obtained with the proposed nonlinear filter.

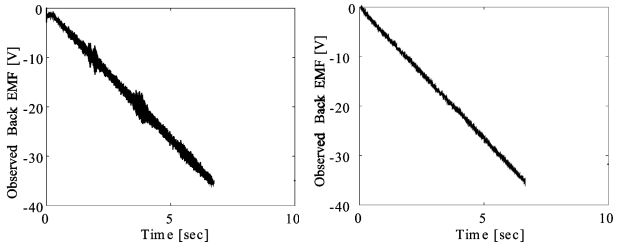

(a) Observed EMF signal with noise (b) Filtered back EMF curve

Fig. 8. Experiment curves obtained with the novel filter.

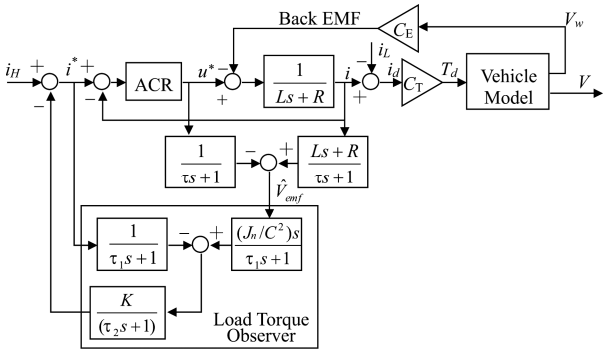

Fig. 9. Slip prevention system based on load the disturbance observer.

As the time constant of the inner loop is more than 10 times smaller than that of the outer loop, in order to simplify dynamic analysis of the system, the transfer function from i^* to i is considered tobe 1. Thus the open loop transfer function from the human drive command i_H to the drive current i_d is

$$G_{OL} = \frac{K}{(\tau_1 s + 1)(\tau_2 s + 1) - K}. \tag{8}$$

Drawing the Bode diagram of the open transfer function as shown in Fig. 10, the dynamics of the system can be analyzed as follows.

The Bode diagram shows that, when $K \le 1$, the gain margin and phase margin are big enough, but when $K > 1$, due to the small stability margin, the system will has poor performance against uncertainty in low and high frequency parts.

The closed loop transfer function from i_H to i_d is

$$G_{CL} = \frac{(\tau_1 s + 1)(\tau_2 s + 1)}{(\tau_1 s + 1)(\tau_2 s + 1) + K(J_n / J - 1)}. \tag{9}$$

This indicates that, under equivalent inertia of the vehicle model $J = J_n$, the closed loop transfer function will be equal to 1; that is, the current command, *i.e.*, the torque command, will be exactly realized by the controller. And if a slip happens, the inertia J will decrease, and the transfer function will also decrease with the change of J. On the other hand, when J increases, the transfer function will also increase to keep the acceleration at a constant value.

Based on this analysis, K should be kept under 1. Under this condition, the controller can maintain the given acceleration, but this may also lead to slips.

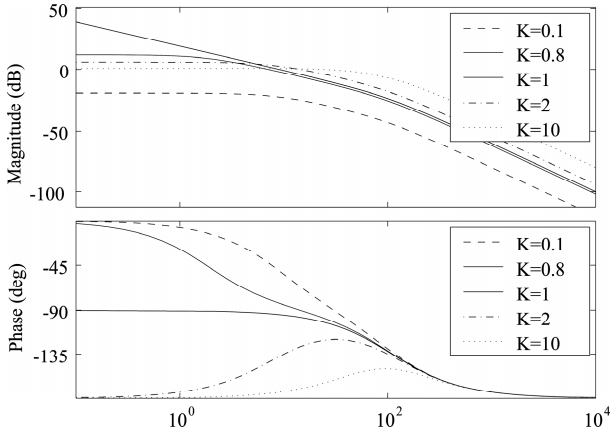

Fig. 10. Bode diagram of the slip controller based on a sload torque observer.

V. SKID PREVENTION CONTROLLER BASED ON ADHESION STATUS ANALYZER

Although the skid prevention controller can limit the torque to some extend when a slip occurs, if the torque command does not decrease, the wheel may slip on a slippy road. Thus, an Adhesion Status Analyzer (ASA) has been designed to solve this problem. The Adhesion Status Analyzer is responsible for observing the friction coefficient, evaluating the adhesion status index, and calculating the maximum safe friction coefficient. Thus, when a slip occurs, the torque command will be limited within the calculated maximum safe acceleration value.

5.1 Friction coefficient observer

According to the equation (1), the load force of the wheel is

$$F_d = (T - \dot{\omega} J_w - F_w(\omega))/r . \quad (10)$$

From Eq. (5) and Eq. (10), the friction coefficient can be calculated as

$$\mu(\lambda) = \frac{T - J_w \dot{\omega} - F_w(\omega) r}{Nr} . \quad (11)$$

If $F_w(\omega)$ is small enough to be ignored, the equation of friction coefficient can be simplified as

$$\mu(\lambda) = \frac{T - J_w \dot{\omega}}{Nr} . \quad (12)$$

In some cases, it is necessary to consider the other forces. Suppose that in the equation of acceleration, that is Eq. (2), the main part of the resistance force $F_V(V)$ is the drag force of the wind, and suppose that

$$F_V(V) = C_d \, Ar \frac{V^2}{2} , \quad (13)$$

where, C_d is the drag coefficient, r is the air density, A is reference area, and V is the vehicle velocity. Because the variables are constant except for the velocity V, the drag force can be written as

$$F_V(V) = C_f V^2 . \quad (14)$$

5.2 Adhesion status index

In the drive mode without slips, when the electric torque T increases, the speed of the wheel also increases. This leads to a bigger speed difference $\Delta V = (V_w - V)$ Thus, the drive force F_d, as well as the velocity of the vehicle, also increases. After the transient process, the working point of the $\mu - \lambda$ curve moves up to reach a new balance point as shown in Fig. 11. And when the working point is near the top point, the same ΔT results in a bigger ΔV, leading to the new balance point. So we can derive the following lemma.

Lemma. Before the working point reaches the maximum point of $(\lambda_{top}, \mu_{max})$, if the torque increases, then the λ must increase, and vice versa.

A wheel-road system can be considered as a geared system. When the slip ratio λ is near zero, the engagement of the gears is good. When λ increases to 1, the engagement status becomes worse; the efficiency of drive transmission also decreases. With the same increase of the electric torque, the force increase occurring on the vehicle side becomes smaller and smaller while the working point moves up along the $\lambda - \mu$ curve. When λ is 1, there is no engaging but rathen sliding friction, which has almost no relation with the electric torque of the wheel side.

Thus, in the adhesion region of $[0, \lambda_{top}]$, the efficiency of drive transmission decreases while the working point moves from (0, 0) to $(\lambda_{top}, \mu_{max})$. And it should exhibit monotonicity before λ reaches λ_{top}.

Based on this analysis, the adhesion status, *i.e.*, the drive transmission status, between the tire and road can be described by the efficiency of drive transmission. The adhesion status index Q can be defined as

$$Q \doteq \frac{F_d V}{T\omega} K_1 . \quad (15)$$

Suppose that before λ reaches λ_{top}, $V \simeq \omega r$, and N is a constant. Then Eq. (15) can be expressed as

$$Q = \frac{\mu}{T} K_1 , \quad (16)$$

where K_1 is a constant, which keeps the index values near 1.

5.3 Maximum safe acceleration

With the value of Q, the position of the working point on the $\lambda - \mu$ curve can be estimated approximately. At the same time, the maximum μ_{max} can be found by judging the value of the adhesion status index Q without calculating the slip ratio λ. Considering a safety factor of μ_{max}, defined as ς,

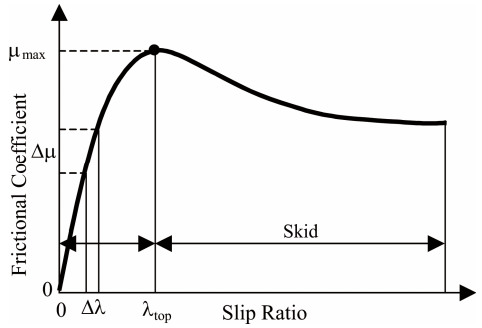

Fig. 11. Analysis of $\lambda - \mu$ curve.

we can get the safe friction coefficient, $\mu_s = \varsigma\mu_{\max}$. Thus, the maximum safe acceleration can be determined as

$$a_{\max} = \frac{N\mu_s}{M}. \tag{17}$$

Then a proper speed pattern can be generated based on the on-line estimated maximum safe acceleration $a_{\max}$.

5.4 Stop distance predictor

Safe braking is an important performance feature of a vehicle, especially in the case of an emergency or slippy road. For this reason, predicting the emergent stop distance under the current road status and current speed can help the driver control the velocity and ensure the safety of the vehicle.

In the Emergent Brake mode, the maximum brake acceleration can be used immediately. The shortest brake time and the shortest brake distance can be expressed as

$$t_{break} = \frac{v}{a_{max}}, \quad d_{break} = \frac{{v_0}^2}{2a_{max}}. \tag{18}$$

5.5 Experimental results of slip prevention with the adhesion status analyzer

Suppose that the vehicle is moving from a dry road onto an icy road, and that the surface of the icy road is very smooth, so that the friction between the tire and the road rapidly decreases. At the same time, if the motor of the EV is still maintaining the driving torque as before, then the wheel will slip on the icy road quickly. The slip phenomenon was simulated using MATLAB for the EV system as shown in Figs. 2 and 9. Suppose the EV starts to accelerate on the dry road at $t = 0$ and that at $t = 3$ sec, it mores onto the icy road. The parameters of the EV system were used with those of "UOT March I." In order to compare simulation result with the experiment, the simulation outputs were proportionally converted into the scope of the experiment results.

In order to show the effect of the skid prevention controller with the Adhesion Status Analyzer (ASA), the system was tested without the Adhesion Status Analyzer and with the Adhesion Status Analyzer under safety factors of 1, 0.75, and 0. The experimental results are shown in Fig. 12. Fig. 12(a) to Fig. 12 (h) show the curves of the wheel speed, chassis speed, torque, acceleration, observed back EMF, friction coefficient, adhesion status index, and slip ratio. The new safety maximum friction coefficient changes when $Q < 0.65$. The comparison proves that the Adhesion status Analyzer can estimate the proper maximum acceleration and that then a new acceleration command can be generated with the new maximum acceleration. The slip ratio can be restrained effectively with the proper safety factor.

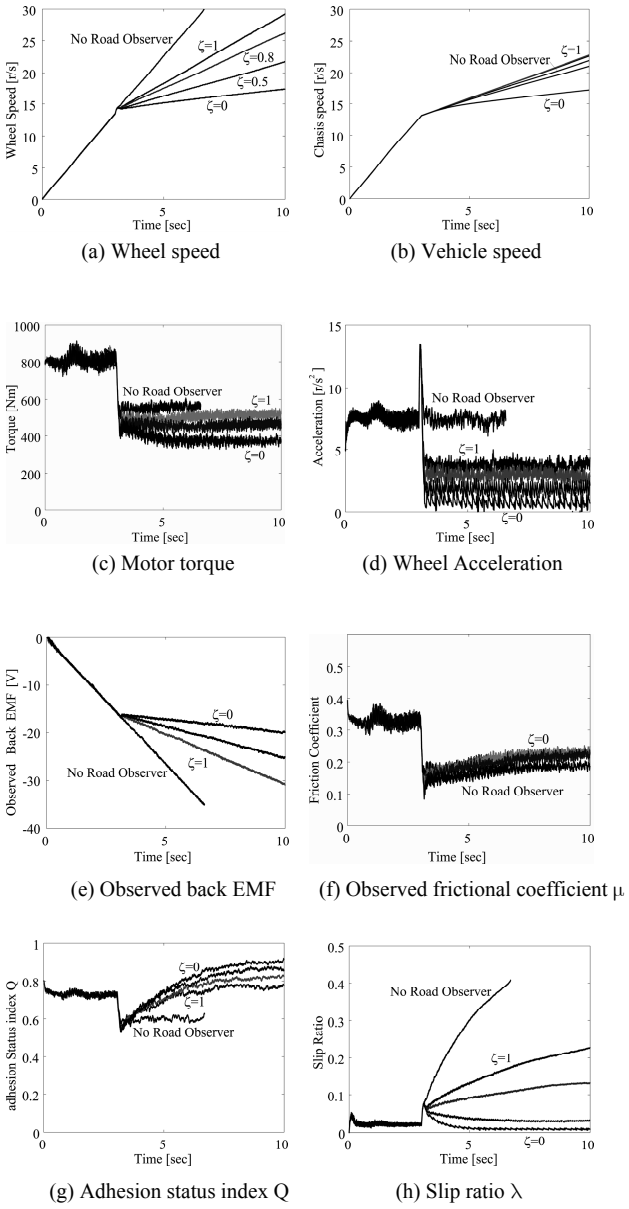

(a) Wheel speed (b) Vehicle speed

(c) Motor torque (d) Wheel Acceleration

(e) Observed back EMF (f) Observed frictional coefficient μ

(g) Adhesion status index Q (h) Slip ratio λ

Fig. 12. Experimental results obtained with skid prevention controller and Adhesion Status Analyzer.

VI. CONCLUSIONS

A comparison of the simulation results and the experiment results shows that the vehicle slip simulator using the M-G setup can be tested easily and that the conditions of the controller and system can adjusted freely. The features of the simulator system are similar to those of a real vehicle. It can be used to verify the slip controller before in-field experiment are performed. With the anti-slip controller and back EMF observer, the system does not need a wheel encoder, and the reliability of the slip prevention controller can be enhanced. The Adhesion Status Analyzer

can be used to help the driver adapt to a slippy road. Its anti-slip performance can be regulated with the safety factor μ_s. The simulation and experiment prove its feasibility and validity.

REFERENCES

1. Hori, Y., Y. Toyoda, and Y. Tsuruoka, "Traction Control of Electric Vehicle: Basic Experimental Results Using the Test EV (UOT Electric March)," *IEEE Trans. Ind. Appl.*, Vol. 34, No. 5, pp. 1131-1138 (1998).
2. Sakai, S. and Y. Hori, "Advantage of Electric Motor for Anti Skid Control of Electric Vehicle," *EPE J.*, Vol. 11, No. 4, pp. 26-32 (2001).
3. Kataoka, S.H., "Optimal Drive Force Control of EV Based on Road Status Observing," Master Dissertation, University of Tokyo (2001).
4. Unsal, C. and P. Kachroo, "Sliding Mode Measurment Feedback Control for Antilock Braking System," *IEEE Trans. Contr. Syst. Technol.*, Vol. 7, No. 2, pp. 271-281 (1999).
5. Yu, F., J.Z. Feng, and J. Li, "A Fuzzy Logic Controller Design for Vehicle ABS with an On-Line Optimized Target Wheel Slip Ratio," *Int. J. Autom.Technol.*, Vol. 3, No. 4, pp. 165-170 (2002).
6. Kodama, S., L. Li, and Y. Hori., "Skid Prevention for EVs Based on the Emulation of Torque Characteristics of Separately-Wound DC Motor," *AMC'04*, Kawasaki, pp. 75-80 (2004).
7. Miyamoto, T. and Y. Hori, "Adhesion Control of EV Based on Disturbance Observer," *IEE Japan Tech. Meet. Rec., IIC-00-9*, pp. 49-54, in Japanese (2000).
8. Shin'ichiro S., S. Hideo, and Y. Hori, "Dynamic Driving/Braking Force Distribution in Electric Vehicle with Independently Driven Four Wheels," *Electr. Eng. Japan*, Vol. 138, No. 1, pp. 79-89 (2002).
9. Li, L., S. Kodama, and Y. Hori, "Back-EMF Based Slip Prevention Controller for EV Simulated by DC Motor System," *Proc. China Contr. Conf.*, pp. 1466-1470 (2004).
10. Hattori, Y., "Optimum Vehicle Dynamics Control Based on Tire Driving and Braking Forces," *R&D Rev. Toyota CRDL*, Vol. 38, No. 4 (2002).
11. Hac, A. and M.D. Simpson, "Estimation of Vehicle Side Slip Angle and Yaw Rate," *Vehicle Dyn. Simul.*, SP-l526 (2000).
12. Beyer, K., E. Krueger, and M. Sonnenberg, "Enhanced Vehicle Stability with Engine Drag Control," *Vehicle Dyn. Simul.*, SP-l656 (2002).
13. Hedrick, J.K., R. Sengupta, Q. Xu, C. Lee, Y.Q. Xu, C. Lee, and Y. Kang, "Enhanced AHS Safety Through the Enhanced AHS Safety Through the Integration of Vehicle Control and Integration of Vehicle," *Contr. Commun.* (2002).